

Analytical Methods

Accepted Manuscript

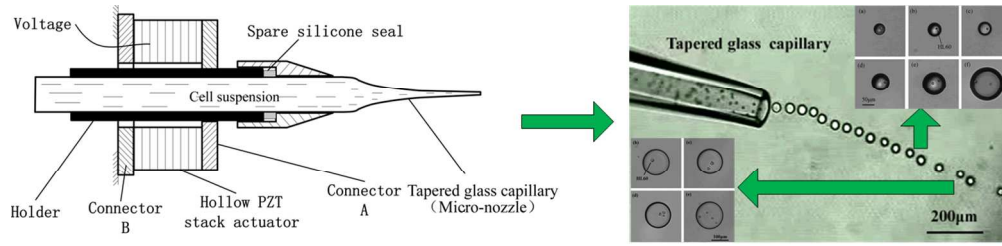


This is an *Accepted Manuscript*, which has been through the Royal Society of Chemistry peer review process and has been accepted for publication.

Accepted Manuscripts are published online shortly after acceptance, before technical editing, formatting and proof reading. Using this free service, authors can make their results available to the community, in citable form, before we publish the edited article. We will replace this *Accepted Manuscript* with the edited and formatted *Advance Article* as soon as it is available.

You can find more information about *Accepted Manuscripts* in the [Information for Authors](#).

Please note that technical editing may introduce minor changes to the text and/or graphics, which may alter content. The journal's standard [Terms & Conditions](#) and the [Ethical guidelines](#) still apply. In no event shall the Royal Society of Chemistry be held responsible for any errors or omissions in this *Accepted Manuscript* or any consequences arising from the use of any information it contains.



191x47mm (192 x 192 DPI)

1
2
3
4
5
6
7
8
9
10
11
12
13
14
15
16
17
18
19
20
21
22
23
24
25
26
27
28
29
30
31
32
33
34
35
36
37
38
39
40
41
42
43
44
45
46
47
48
49
50
51
52
53
54
55
56
57
58
59
60

1
2
3
4 **A novel approach for encapsulating cells into monodisperse**
5 **picolitre droplets actuated by microfluidic pulse inertia force**
6
7
8

9 **Hongcheng Wang^{1*}, Weiyi Zhang², Zhendong Dai¹**

10
11 ¹ Institute of Bio-inspired Structure and Surface Engineering, Nanjing University of
12 Aeronautics and Astronautics, Nanjing, Jiangsu, China
13
14

15
16 ² School of Mechanical Engineering, Nanjing University of Science and Technology,
17 Nanjing, Jiangsu, China
18
19
20
21
22
23
24
25
26
27
28
29
30
31
32
33
34
35
36
37
38
39
40
41
42
43
44
45
46
47
48
49
50
51
52
53
54
55
56
57
58
59
60

*corresponding author. Tel: +86 25 84892584. Fax: +86 25 84892584-101.

E-mail addresses: whch31@163.com (H.C. Wang)

Abstract

Encapsulation of few cells into monodisperse picolitre droplets is an extremely critical step in the process of the droplet based single cell analysis. This paper presents a novel approach, not based on micro-fluidic chip fabricated by standard soft lithography technique, for encapsulating cells into droplets actuated by microfluidic pulse inertia force. The principle of the encapsulating process is to actuate a hollow PZT stack by a signal generator and a voltage amplification to provide an enough pulse inertia force for a tapered glass capillary and the cell suspension inside to eject droplets in mineral oil and a certain number of the cells will be randomly encapsulated in monodisperse picolitre droplets. The tapered glass capillary was fabricated by glass heating process without complicated microfabrication technology. So it has the advantages of good chemical resistance, low friction, easy to manufacture and low cost. The minimum size of the spherical cell droplets can be reached is 20 μm in diameter and about 4 picolitre in volume. The percentage of the droplets with single HL60 cell can reach 42% when the droplet size is 40 μm and the concentration of the cell suspension is 1×10^8 cells per milliliter since the alternate changed pulse inertia force can make the cells well dispersed in the tapered capillary. The percentage of viable cells can be reached is 82% as determined by Trypan Blue staining when the cell droplet size is 120 μm . The experiment results present a novel strategy for droplet-based single cell analysis.

Keywords: microfluidics; droplet; PZT actuator; cell encapsulation; cell analysis;

1 Introduction

In recent years, as a subcategory of microfluidics, droplet-based microfluidics has made great process and its application in single cell analysis has attracted more and more attention^{1, 2, 3}. Droplet-based single cell analysis is a method of encapsulating single cell, reagent and reaction product in a small droplet to analyze dynamic behavior⁴, directed evolution of enzymes⁵, protein crystallization⁶, polymerase chain reaction⁷ and gene detection⁸ and gene expression⁹ of single cells. In the droplet-based single cell analysis, each cell can be made to reside within its own picolitre-volume drop, chemically isolated from all the other drops, cell-secreted molecules rapidly achieve detectable concentrations in the confined fluid surrounding the encapsulated cell¹⁰.

The vast majority of reported methods of encapsulating single cells into monodisperse picolitre droplets are based on micro-fluidic chip. In the micro-fluidic chips, T-junction^{11, 12} and flow-focusing configuration^{13, 14, 15} are frequently adopted, the shearing force of one flowing fluid against another is used and droplets are continuously generated utilizing the oil-aqueous interface instability. In the above two shear-flow-driven droplet generators, microfluidic devices (or microfluidic chips) usually fabricated with polydimethylsiloxane (PDMS) using the standard soft lithography technique are necessary^{16, 17, 18}. The fluids are usually driven by syringe pumps and the size of the cell droplets can be changed by altering the fluid flow rates, the channel widths, or the relative viscosity between the two phases¹⁹. So, the process of loading cells into drops is purely random, the distribution is dictated by Poisson statistics²⁰. To control the number of cells in droplets, Edd et al. designed a flow-focusing microfluidic chip with high aspect-ratio microchannels to controllably load cells into drops because the high aspect-ratio microchannels can cause cells to self-organize into two evenly-spaced streams²¹.

The other reported encapsulating methods include droplet assembling technique and cell printing technology, which are not based on micro-fluidic chip. Droplet assembling technique^{22, 23} uses a capillary sampling probe and array of horizontally

1
2
3
4 positioned micro-sample vials with a slot fabricated on the bottom of each vial. The
5 cell suspension and the oil are in different vials, which the capillary sampling probe
6 dips into successively. The method has high controllability on the compositions and
7 volumes of droplets in the nanoliter to picolitre range. Cell printing technology uses
8 droplet generators in gaseous environments ²⁴ to place single cells encapsulated in
9 picolitre volume on “drop-on-demand” mode to a desired location. The reported
10 droplet generators mainly include pneumatically actuated droplet generator ²⁵ and
11 acoustically actuated droplet generator ²⁶. The droplets encapsulated with single cells
12 ejected by cell printing technology are usually prepared for tissue printing and tissue
13 engineering ^{27,28}.

24 In our previous work, based on microfluidic pulse inertia force we have
25 developed a drop-on-demand droplet generator for ejecting droplets of low viscosity
26 liquid in gaseous environment ²⁹ and applied it to fabrication of micropellistor ³⁰,
27 paper micro-fluidic device ³¹ and PDMS microfluidic device ³². Herein, based on
28 microfluidic pulse inertia force, we developed a novel cell encapsulating approach
29 without micro-fluidic chips. The droplets of cell suspension are ejected from a tapered
30 glass capillary actuated by a hollow PZT stack, without the need of special
31 microchannel networks or external devices.

41 **2 Experiment**

42 *2.1 Reagents and materials*

45 Human leukemia cell (HL60) was supplied by Shanghai Meixuan Biological
46 Science and Technology LTD. RPMI1640 culture medium was purchased from
47 Shanghai BioSun Sci&Tech CO., LTD. Mineral oil (M5904) was purchased from
48 American Sigma-Aldrich Company. Span 80 was purchased from Tianjin Hengxing
49 Chemical Preparation Co., Ltd. Trypan Blue was purchased from Beyotime Institute
50 of Biotechnology.

51 *2.2 Experiment apparatus*

52 In Fig.1 (a), the assembly of the picolitre cell droplet generator based on
53 microfluidic pulse inertia force is shown. The structure of the generator mainly
54
55
56
57
58
59
60

1
2
3
4 consists of five parts: (1) tapered glass capillary, (2) capillary holder, (3) hollow PZT
5 stack actuator, (4) connector A and (5) connector B. The tapered capillary (usually
6 referred as micro-nozzle) clamped by the capillary holder, which is fixed with the
7 right face of the hollow PZT stack actuator (WTYDCR, CETC) through connector A
8 while the left face is fixed with body frame and kept stationary through connector B.
9 So, the right and left face of the actuator are called movable and stationary face
10 respectively. There are neither micro pumps nor micro valves, which have either
11 micro moving parts or embedded micro electric circuits, therefore significantly
12 simplifying the structure, and decreasing the difficultness in manufacturing and the
13 cost of the generator.
14
15
16
17
18
19
20
21
22
23

24 The hollow PZT stack actuator is constructed of several disc-shaped
25 piezoelectric ceramic pieces, the thickness of which is in the range of 0.02~1 mm.
26 There is an approximate linearity between applied voltage amplitude and the right
27 face displacement of the actuator. So, the actuator will cause a larger displacement
28 instantaneously and consequently provide a greater pulse inertia force for the
29 micro-nozzle and cell suspension inside when a higher pulse driving voltage is
30 applied. Fig. 1(b) shows the typical waveform of the driving signal and T is the
31 driving period. The frequency of driving signal is variable from 2~256 Hz.
32
33
34
35
36
37
38
39

40 Glass material was chosen to make the tapered glass capillary because of several
41 advantages, such as good chemical resistance, low friction, easy to manufacture and
42 low cost. The raw material is borosilicate glass capillary (Beijing Zhengtiany
43 Scientific And Trading Co., Ltd.). The dimensions of glass capillary are 1.6 mm, 1.0
44 mm and 100 mm in external diameter, internal diameter and length, respectively.
45 Glass heating process was adopted to fabricate the micro-nozzle without complicated
46 microfabrication technology and can be divided into two steps: (1) pulling a capillary
47 to form a micro-nozzle with straight outlet and (2) forging the straight outlet to form a
48 shrinkage one. The detail fabrication process for the micro-nozzle was presented in
49 literature³⁰. The micro-nozzles with different outlet diameters can be obtained by
50 varying the control parameters of the voltage amplitude and the balance weights (The
51 outlet diameter in this article means the inner diameter of the nozzle tip). The
52
53
54
55
56
57
58
59
60

1
2
3
4 minimum outlet diameter of the fabricated micro-nozzle can reach as small as 10 μm .
5
6 The fabricated micro-nozzle with outlet diameter of 40 μm is shown in Fig.1 (c).

7 8 *2.3 Process of encapsulating cells into droplets*

9
10 The driving mechanism of cell droplets formation in the mineral oil actuated by
11 microfluidic pulse inertia force is shown in Fig.2. When being applied with a pulse
12 voltage, the PZT actuator stretches and exerts a driving force F_1 on the solid wall of
13 the glass micro-nozzle through the connector A. In consequence, the glass solid wall
14 and the boundary flow obtains a movement along with the nozzle axis. Then the
15 viscous force V_1 within the cell suspension liquid transfers the movement and the
16 microfluidic body obtains a velocity v . When the applied pulse voltage decreases
17 rapidly to zero in magnitude, the PZT actuator contracts and the liquid inside the
18 micro-nozzle obtains a pulse inertia force F_2 relative to the micro-nozzle. When the
19 inertia force F_2 is small in magnitude, the viscous forces V_2 within the liquid is greater
20 than the inertia force F_2 , the liquid will move along with the nozzle, while, when the
21 inertia force F_2 is larger enough in magnitude, the inertia force F_2 exceeds the viscous
22 force V_2 , a droplet of the cell suspension will be thrown out of the micro-nozzle drop
23 by drop in the direction of the inertia force F_2 in aid of the shear force $F\tau$ from the
24 mineral oil. The influence of pulse voltage waveform on the acceleration of
25 micro-channel solid wall, microfluidic pulse inertia force and driving effect of
26 microfluids had been researched in literature³³ and the waveform in Fig.1 (b) can
27 produce a bigger microfluidic pulse inertia force which is more beneficial to droplet
28 formation.
29
30
31
32
33
34
35
36
37
38
39
40
41
42
43
44
45
46
47

48 *2.4 Encapsulation of cells in picolitre droplets*

49
50 As is shown in Fig.1 (d), a cell encapsulation experimental apparatus was
51 established, the core component of which is the cell droplet generator actuated by
52 microfluidic pulse inertia force. The pressure regulator is used to produce a small
53 negative pressure in the micro-nozzle and make the micro-nozzle inhaled a certain
54 amount of cell suspension liquid. The droplet generator is fixed on a three-dimension
55 adjusting frame through the connector B. The micro-nozzle orifice is immersed in the
56 mineral liquid in a watch glass, which is placed on the stage of a chatelier-type
57
58
59
60

1
2
3
4 microscope (TS-100, Nikon).

5
6 In the experiment, Human leukemia cell (HL60) with concentration from
7 1.0×10^7 to 1.0×10^8 cells per milliliter is used. HL60 is a kind of suspension cell,
8 which is normally used in the research of single cell encapsulation. Fig.3 (b) shows
9 the micrograph of HL60 cells with concentration of 1.0×10^7 cells per milliliter on a
10 glass slide. The diameter of the cells is in the range of 6~12 μm and the average
11 diameter is about 8 μm . Mineral oil was added with 10% span 80, a kind of surfactant,
12 to prevent the generated cell droplets from being fused.
13
14
15
16
17
18
19

20 In an additional experiment, we assessed the effect of the applied voltage
21 amplitude and cell droplet size on the cell survival rates which was detected by
22 Trypan Blue Staining. The cell suspension was added with 50% Trypan Blue. So, both
23 of the cells and Trypan Blue would be encapsulated in a droplet. The cell survival rates
24 could be counted in the chatelier-type microscope in three minutes.
25
26
27
28
29
30

31 **3 Results and Discussion**

32
33 As is shown in Fig.3 (a), the cell droplets were ejected from a tapered capillary
34 with outlet diameter of 80 μm actuated by microfluidic pulse inertia force in mineral
35 oil environment. One cell droplet will be produced in a pulse driving period. In other
36 words, the droplet formation frequency is equal to the frequency of driving signal ($1/T$,
37 shown in Fig.1 (b)), which is 2~256 Hz. So, the maximum rate of droplet generation
38 can be reached is 256 droplets per second. Besides that, the microfluidic pulse inertia
39 force produced by the hollow PZT stack actuator makes the cells uniformly dispersed
40 in the micro-nozzle before being ejected. This is because the direction of pulse inertia
41 force is of alternate change and can make the cell suspension in the micro-nozzle
42 oscillate slightly. The well dispersion of cells is beneficial to the uniformity of cell
43 numbers in droplets. The number of the cells encapsulated in droplets is random and
44 may be zero, one, two or three, as is shown in Fig.3 (c).
45
46
47
48
49
50
51
52
53
54
55
56

57 The generation of cell droplets is actuated by microfluidic pulse inertia force
58 produced by a piezoelectric actuator, so the size of the droplets is determined mainly
59 by the tapered capillary outlet diameter and frequency, amplitude of the applied pulse
60

1
2
3
4 voltage with the invariable of the voltage waveform. Fig.4 (a) shows the variation of
5 cell droplet size with the voltage amplitude for different diameters of capillary outlets.
6 The frequency of the applied voltage is set at a lower value of 2 Hz. Each data point is
7 an average of ten measurements. The hollow PZT stack actuator causes a larger
8 displacement instantaneously and consequently provides greater pulse inertia force for
9 the tapered capillary and cell suspension inside when a higher driving voltage is
10 applied. So, cell suspension will be ejected drop by drop and the droplet size will
11 increase when the voltage amplitude rises. If the voltage is low in magnitude, cell
12 droplets won't be ejected when the micro-nozzle size is relatively small. For instance,
13 the minimum voltage to eject droplets is 20 V for nozzle orifice diameters of 20 μm .
14 On the other hand, when the voltage amplitude is relatively high, the inertia force was
15 big enough to eject more mass of liquid, maybe forming satellite droplets. For
16 instance, the maximum voltage to stably eject droplets without satellite droplets is 50
17 V when the capillary orifice diameter is 100 μm .

18
19
20
21
22
23
24
25
26
27
28
29
30
31
32 As is shown in Fig.4 (b), the cell droplet size decreased with the increase of the
33 voltage frequency under different voltages. In Fig.4 (b), the diameter of nozzle outlet
34 is set as 60 μm . However, when the voltage frequency is above 30 Hz, the droplets
35 cannot be generated with the voltage amplitudes of 70 V. The reason is that it needs
36 time for PZT stack actuator to have a response to the driving voltage signal. If the
37 voltage amplitude is too high, the actuator will produce a larger displacement and the
38 response time is relatively long, which will cause interference between the
39 neighboring driving voltage periods and the produced pulse inertia force is not big
40 enough to form droplets. The standard deviation of the cells droplets can be obtained
41 and is less than 5%. These HL60 cells were 6~12 μm in diameter in culture whereas
42 the generated droplets were in the range of 20~130 μm in diameter. So, the non
43 uniform size of the cells has little influence on the monodispersity of the fabricated
44 droplets because the cell is much smaller than the droplets. The cell droplets with
45 different sizes are shown in Fig.5.

46
47
48
49
50
51
52
53
54
55
56
57
58
59
60
The number of the cells encapsulated in droplets is random. It is the concentration of the cell suspension and the droplet size that determined the average

1
2
3
4 number of cells in a droplet. Fig.6 (a) shows the variation of single cell droplet
5 percentage with concentration of the cell suspension for different droplet sizes. Each
6 presented data point represents an analysis of 200 droplets observed by a
7 chatelier-type microscope. If the cell density of the suspension is relatively low
8 (below 6×10^7 cells per milliliter), the fraction of droplets with single cell decreases
9 with the increase of the droplet size and the fraction is relatively low (below 25%),
10 because the number of the cells is too small and a large number of the droplets
11 encapsulating no cells.
12

13
14
15
16
17
18
19
20 If the cell density of the suspension is relatively high (above 6×10^7 cells per
21 milliliter), the fraction of droplets with single cell reaches maximum. For instance,
22 when the cell density is 1×10^8 cells/mL and if the droplet size is too small (below
23 $40 \mu\text{m}$) there will be a large number of droplet encapsulating two, three or four cells
24 and the fraction of single cell droplet is not large enough. The droplets capsulating
25 different numbers of cells are shown in Fig.6 (b) ~ (e). When the droplet size is $40 \mu\text{m}$
26 with the concentration of the HL60 cell suspension being 1×10^8 cells per milliliter, the
27 fraction of droplets with single cell obtains the maximum value of 0.42.
28
29

30
31
32
33
34
35
36 In the additional experiment of cell viability, the percentage of viable cells
37 decreased slowly with the increase of driving voltage amplitude when the cell droplet
38 size was controlled as $80 \mu\text{m}$ by adjusting the two parameters of the tapered nozzle
39 outlet diameter and voltage frequency, as is shown in Fig.7 (a). Each presented data
40 point represents an analysis of 100 cells observed by a chatelier-type microscope. The
41 outlet diameter of the tapered nozzle (D) and voltage frequency (f) are shown on the
42 top of each data point in Fig.7 (a). The higher applied pulse voltage amplitude causes
43 a larger microfluidic pulse inertia force and a high shear stress which may have an
44 influence on the cell viability. Despite this, the percentage of viable cells is above 75%
45 when the driving voltage amplitude is as high as 70 V.
46
47
48
49
50
51
52
53
54
55

56 The percentage of viable cells increased with the increase of the cell droplet size,
57 as is shown in Fig.7 (b). The droplet sizes range from $20 \mu\text{m}$ to $120 \mu\text{m}$ were
58 controlled by adjusting the two parameters of the tapered nozzle outlet diameter (D)
59 and voltage amplitude (U) while the voltage frequency (f) was set as 2Hz. The two
60

1
2
3
4 parameters are shown on the top of each data point in Fig.7 (b). The experiment result
5 indicates that increasing the amount of the cell nutrient solution in a single droplet can
6 prevent the cells from being damaged by the pulse inertia force or shear stress and is
7 benefit to the cell viability consequently. The percentage of viable cells can be
8 reached is 82% as determined by Trypan Blue staining when the cell droplet size is
9 120 μm . After being stained by Trypan Blue, the living cell has an intact cell
10 membrane while the dead cell has a destroyed membrane and its shape is irregular.
11 The micrographs of the living cell and dead cell are shown in Fig.7 (c) and Fig.7 (d)
12 respectively.
13
14
15
16
17
18
19
20
21
22

23 **4 Conclusions**

24
25 In summary, this paper introduced a new approach for encapsulating cells into
26 monodisperse picolitre droplets actuated by microfluidic pulse inertia force. Different
27 from the existent technology, this method does not need micro-fluidic chip fabricated
28 by standard soft lithography technique. A hollow PZT stack is used to provide enough
29 pulse inertia force for a tapered glass capillary and the cell suspension inside to eject
30 droplets in mineral oil and a certain number of the cells will be randomly
31 encapsulated in the droplets. The tapered glass capillary was fabricated by glass
32 heating process without complicated microfabrication technology. So it has the
33 advantages of good chemical resistance, low friction, easy to manufacture and low
34 cost and it won't destroy the cells and other biological reagents during encapsulating
35 process. The cell droplet sizes range from 20 μm to 130 μm and can be precisely
36 controlled by changing the capillary outlet diameter and the frequency, amplitude of
37 the pulse voltage signal applied on the hollow PZT stack actuator. The percentage of
38 the droplets with single HL60 cell can be reached is 42% when the droplet size is 40
39 μm and the concentration of the cell suspension is 1×10^8 cells per milliliter since the
40 alternate changed pulse inertia force can make the cells well dispersed in the
41 micro-nozzle. The percentage of viable cells can reach 82% as determined by Trypan
42 Blue staining when the cell droplet size is 120 μm .
43
44
45
46
47
48
49
50
51
52
53
54
55
56
57
58
59
60

Acknowledgement

The work was supported by Postdoctoral Science Foundation of China (no. 2014M551584) and National Natural Science Foundation of China (no. 51175268, no. 11102090).

Reference

- 1 S.Y. Teh, R. Lin, L.H. Hung, A.P. Lee. *Lab Chip*, 2008, 8, 198-220.
- 2 M. Margulies, M. Egholm, W. E. Altman, S. Attiya, J.S. Bader, L. A. Bembien. *Nature*, 2005, 437, 376-380.
- 3 H.Song, D.L. Chen, R.F. Ismagilov. *Angew. Chem.Int.Ed.*, 2006, 45, 7336-7356.
- 4 M.A. Khorshidi, P.K.P. Rajeswari, C.Wählby, H.N. Joensson, H.A. Svahn. *Lab Chip*, 2014, 14, 931-937.
- 5 S.L. Sjostrom, Y.P. Bai, M.T. Huang, Z.H. Liu, J. Nielsen, H.N. Joensson, H.A. Svahn. *Lab Chip*, 2014, 14, 806-813.
- 6 B.Zheng, J.D. Tice, L.S. Roach, R.F. Ismagilov. *Angew. Chem. Int. Ed.* 2004, 43, 2508-2511.
- 7 D.Y. Liu, G.T. Liang, X.X. Lei, B. Chen, W.Wang, X.M. Zhou. *Anal. Chim. Acta.*, 2012, 718, 58-63.
- 8 T.D. Rane, H.C. Zec, C.Puleo, A.P. Lee, T.H. Wang. *Lab chip*, 2012, 12, 3341-3347.
- 9 P. Mary, L. Dauphinot, N. Bois, M.C. Potier, V. Studer, P. Biomicrofluidics, 2011, 5, 024109.
- 10 S. Lindstrom, H.A. Svahn. *Lab chip*, 2010, 10, 3363-3372.
- 11 T. Thorsen, R.W. Robert, F.H. Arnold, S.R. Quake. *Phys. Rev. Lett.*, 2001, 86, 4163-4166.
- 12 H. Yang, Q. Zhou, L.S. Fan. *Chem. Eng. Sci.*, 2013, 87, 100-110.
- 13 S.L. Anna, N. Bontoux, H.A.Stone. *Appl. Phys. Lett.*, 2003, 82, 364-366.
- 14 T.T. Fu, Y.N. Wu, Y.G. Ma, H.Z. Li. *Chem. Eng. Sci.*, 2012, 84, 207-217.
- 15 A.Gupta, H.S. Matharoo, D. Makkar, R. Kumar. *Computers & Fluids*, 2014, 100, 218-226.
- 16 S. Mazzitelli, L. Capretto, F. Quinci, R. Piva, C. Nastruzzi. *Adv. Drug. Deliver. Rew.*, 2013, 65, 1533-1555.
- 17 A. Kang, J. Park, J. Ju, G.S. Jeong, S.H. Lee. *Biomaterials*, 2014, 35, 2651-2663.
- 18 J.C. Tormos, D. Lieber, J.C. Baret, A. Harrak, O.J. Miller, L. Frenz, J. Blouwolff, K.J. Humphry, S. Köster, H. Duan, C. Holtze, D.A. Weitz, A.D. Griffiths, C.A.

- 1
2
3
4 Merten. *Chemistry & Biology*, 2008, 15, 427-437.
- 5
6 19 Y. Shi, G.H. Tang, H.H. Xia. *Computers & Fluids*, 2014, 90, 155-163.
- 7
8 20 A.R. Abate, C.H. Chen, J.J. Agresti, D.A. Weitz. *Lab Chip*, 2009, 9, 2628-2631.
- 9
10 21 J.F. Edd, D.D. Carlo, K.J. Humphry, S. Koster, D. Irimia, D.A. Weitz, M. Toner.
11 *Lab Chip*, 2008, 8, 1262-1264.
- 12
13 22 S.Q. Gu, Y.X. Zhang, Y. Zhu, W.B. Du, B. Yao, Q. Fang. *Anal. Chem.*, 2011, 83,
14 7570-7576.
- 15
16 23 W.B. Du, M. Sun, S.Q. Gu, Y. Zhu, Q. Fang. *Anal. Chem.*, 2010, 82, 9941-9947.
- 17
18 24 P.B. Tzvi, W. Rone. *Microsyst Technol*, 2010, 16, 333-356.
- 19
20 25 U. Demirci, G. Montesano. *Lab Chip*, 2007, 7, 1428-1433.
- 21
22 26 U. Demirci, G. Montesano. *Lab Chip*, 2007, 7, 1139-1145.
- 23
24 27 V. Mironov, R.P. Visconti, V. Kasyanov, G. Forgacs, C.J. Drake, R.R. Markwald.
25 *Biomaterials*, 2009, 30, 2164-2174.
- 26
27 28 R.A. Rezendea, F.D.A.S. Pereira, V. Kasyanov, D.T. Kemmoku, I. Maia, J.V.L.
28 *Silvaa*, V. Mironova. *The First CIRP Conference on Biomanufacturing*, 2013,
29 276-281.
- 30
31 29 W.Y.Zhang, L.Y.Hou, China: ZL03152948. 8, 2006. (in Chinese)
- 32
33 30 H.C. Wang, L.Y. Hou, W.Y. Zhang. *Sens. Actuators B*, 183(2013) 342-349.
- 34
35 31 Z.A. Li, L.Y. Hou, W.Y. Zhang, L.Zhu. *Anal. Methods*, 2014, 6, 878-885.
- 36
37 32 Z.A. Li, L.Y. Hou, W.Y. Zhang, L.Zhu. *Anal. Methods*, 2014, 6, 4716-4722.
- 38
39 33 H.C. Wang, L.Y. Hou, W.Y. Zhang. *Opt. Precision Eng.* 2012, 2, 2251-2259.
- 40
41
42
43
44
45
46
47
48
49
50
51
52
53
54
55
56
57
58
59
60

Figure legend

Fig.1 Experimental apparatus: (a) sketch and photo of the droplet generator actuated by microfluidic pulse inertia force, (b) typical waveform of the driving signal on the hollow PZT stack actuator, (c) micrograph of the tapered glass capillary with outlet diameter of 40 μm fabricated by glass heating process and (d) sketch of the whole experimental system for encapsulating single cells in picolitre droplets

Fig.2 Driving mechanism of cell droplets formation in an oil phase liquid actuated by microfluidic pulse inertia force

Fig.3 Encapsulating process of HL60 cells in picolitre droplets actuated by microfluidic pulse inertia force: (a) integrated graph of the encapsulating process, (b) micrograph of human leukemia cell (HL60) suspension with concentration of 1.0×10^7 cells per milliliter and (c) detail with enlarged scale of the encapsulating process

Fig.4 (a) Variation of cell droplet size with voltage amplitude for different diameters of tapered capillary outlet when the voltage frequency is 2 Hz and (b) Variation of cell droplet size with voltage frequency for different voltage amplitudes when the outlet diameter of the tapered capillary is 60 μm

Fig.5 Micrograph of picolitre droplets encapsulating single cells with different droplet sizes of: (a) 40 μm , (b) 45 μm , (c) 50 μm , (d) 60 μm , (e) 70 μm and (f) 110 μm

Fig.6 (a) Variation of single cell droplet percentage with density of the cell suspension for different droplet sizes and Micrograph of picolitre droplets encapsulating (b) single cell, (c) two cells, (d) three cells and (e) four cells

Fig.7 Cell Viability of cells encapsulated in picolitre droplets actuated by microfluidic pulse inertia force: (a) the percentage of viable HL60 cells at different driving voltage amplitudes, (b) the percentage of viable HL60 cells at different droplet sizes, (c) micrograph of the living cell after being stained by Trypan Blue and (d) micrograph of the dead cell after being stained by Trypan Blue

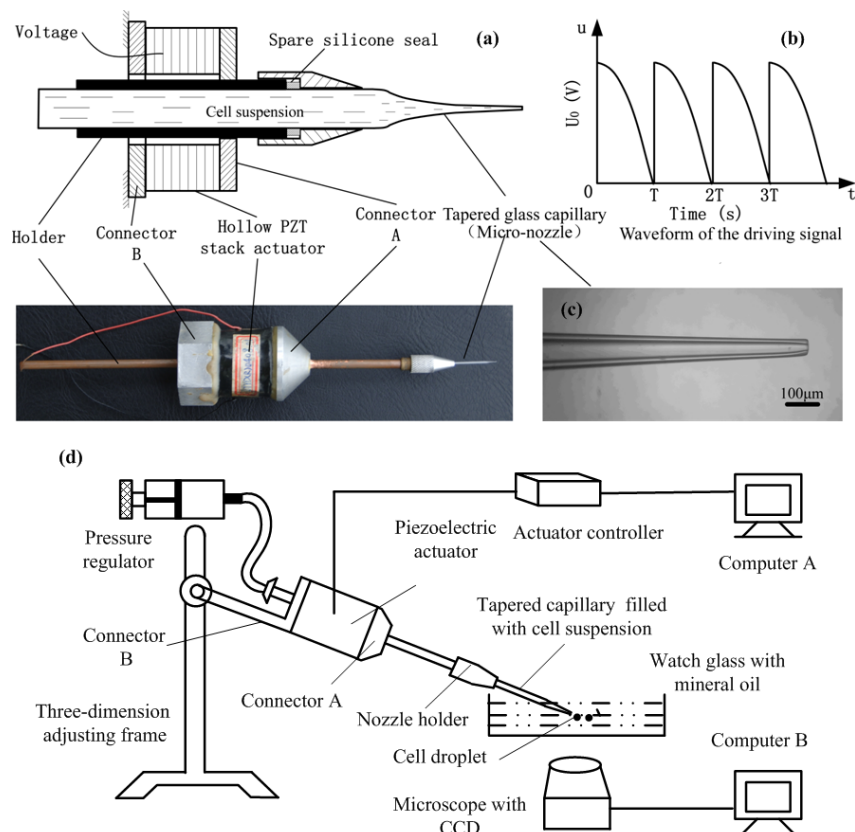


Fig.1 Experimental apparatus: (a) sketch and photo of the droplet generator actuated by microfluidic pulse inertia force, (b) typical waveform of the driving signal on the hollow PZT stack actuator, (c) micrograph of the tapered glass capillary with outlet diameter of $40\ \mu\text{m}$ fabricated by glass heating process and (d) sketch of the whole experimental system for capsulating single cells in picolitre droplets

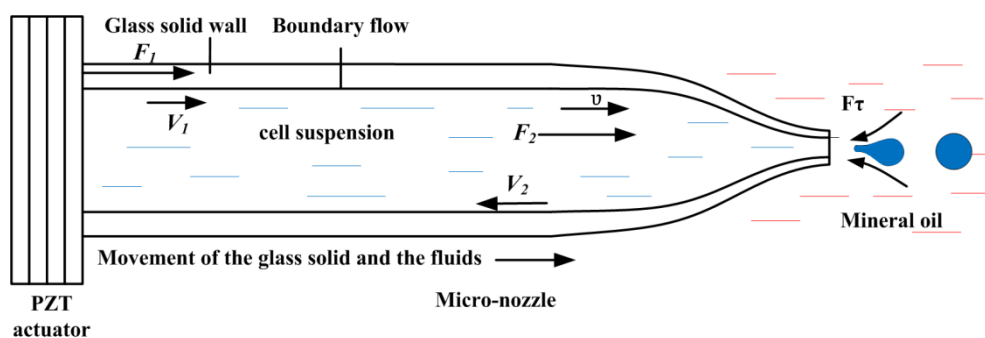


Fig.2 Driving mechanism of cell droplets formation in an oil phase liquid actuated by microfluidic pulse inertia force

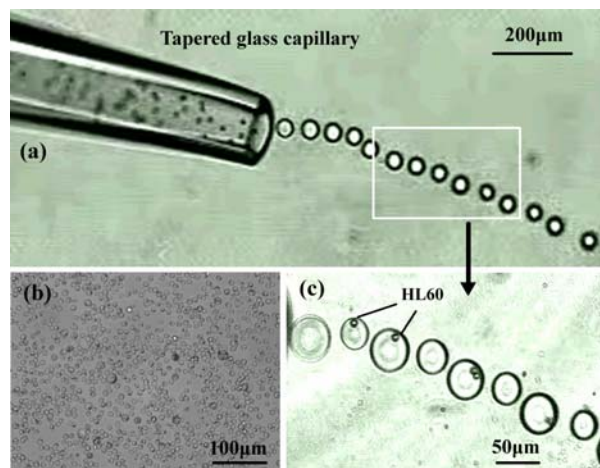


Fig.3 Encapsulating process of HL60 cells in picolitre droplets actuated by microfluidic pulse inertia force: (a) integrated graph of the encapsulating process, (b) micrograph of human leukemia cell (HL60) suspension with concentration of 1.0×10^7 cells per milliliter and (c) detail with enlarged scale of the encapsulating process

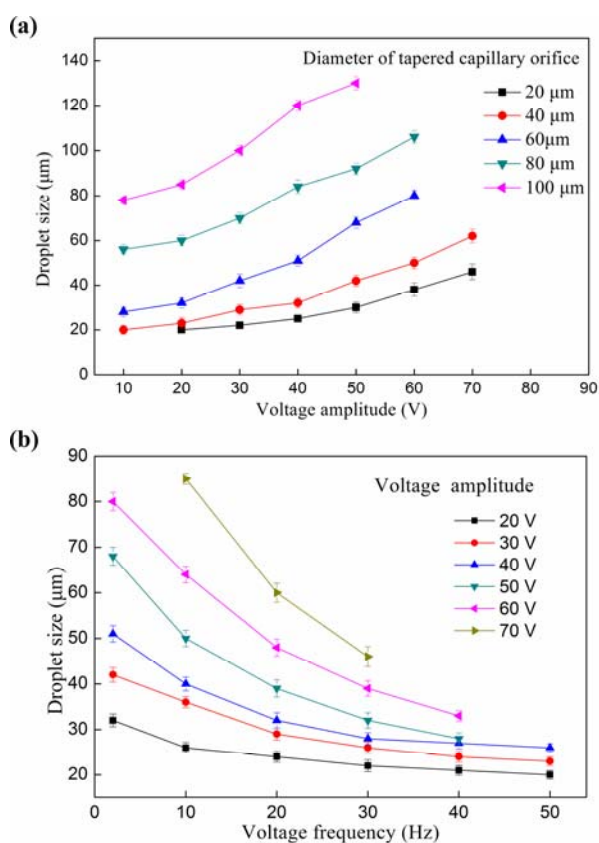


Fig.4 (a) Variation of cell droplet size with voltage amplitude for different diameters of tapered capillary outlet when the voltage frequency is 2 Hz and (b) Variation of cell droplet size with voltage frequency for different voltage amplitudes when the outlet diameter of the tapered capillary is 60 μm

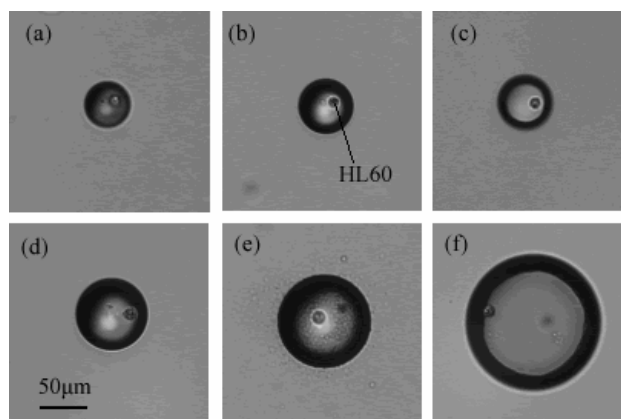


Fig.5 Micrograph of picolitre droplets encapsulating single cells with different droplet sizes of: (a) 40 μm , (b) 45 μm , (c) 50 μm , (d) 60 μm , (e) 70 μm and (f) 110 μm

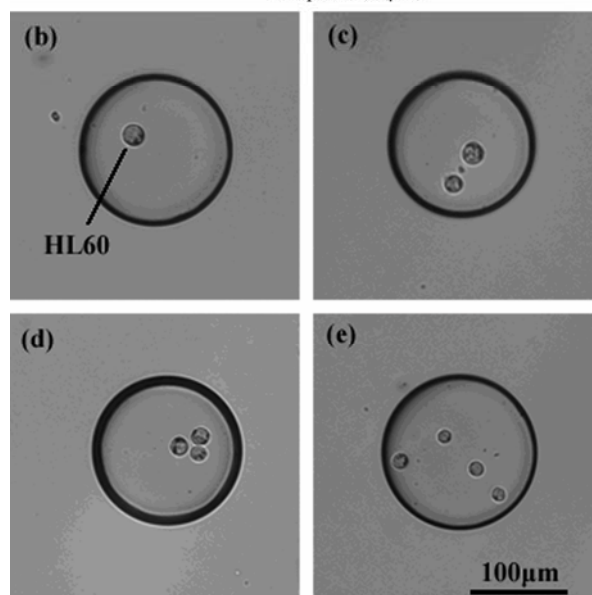
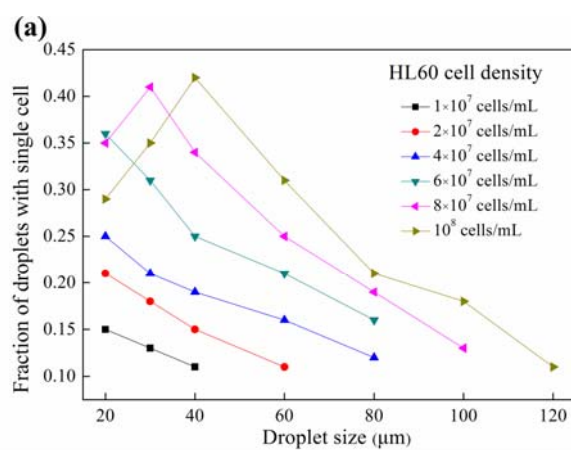


Fig.6 (a) Variation of single cell droplet percentage with density of the cell suspension for different droplet sizes and Micrograph of picolitre droplets encapsulating (b) single cell, (c) two cells, (d) three cells and (e) four cells

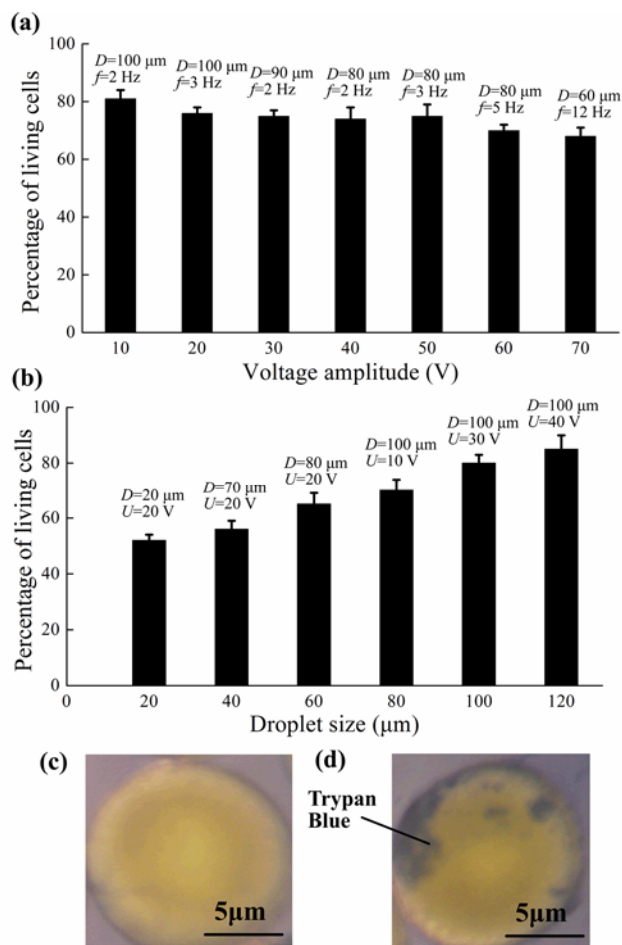


Fig.7 Cell Viability of cells encapsulated in picolitre droplets actuated by microfluidic pulse inertia force: (a) the percentage of viable HL60 cells at different driving voltage amplitudes, (b) the percentage of viable HL60 cells at different droplet sizes, (c) micrograph of the living cell after being stained by Trypan Blue and (d) micrograph of the dead cell after being stained by Trypan Blue